Available online at www.sciencedirect.com
SCIENCE DIRECT
Earth and Planetary Science Letters 248 (2006) 462–475
EPSL
www.elsevier.com/locate/epsl

Sr/Ca and $\delta^{18}O$ seasonality in a *Porites* coral from the MIS 9 (339–303 ka) interglacial

Bridget F. Ayling [a,*], Malcolm T. McCulloch [a], Michael K. Gagan [a], Claudine H. Stirling [b], Morten B. Andersen [b], Steve G. Blake [c]

[a] *Research School of Earth Sciences, The Australian National University, Canberra, ACT 0200, Australia*
[b] *Institute of Isotope Geochemistry and Mineral Resources, ETH-Zentrum, 8092 Zürich, Switzerland*
[c] *ANZLIC—the Spatial Information Council, Level 1, 115 Canberra Ave., Griffith, ACT 2603, Australia*

Received 27 October 2005; received in revised form 7 June 2006; accepted 7 June 2006
Available online 18 July 2006
Editor: M.L. Delaney

Abstract

Past changes in the seasonal distribution of insolation across the Earth's surface are thought to play a critical role in Quaternary climate cycles. In this study we use Sr/Ca and $\delta^{18}O$ as geochemical proxies in the skeleton of a fossil *Porites* coral to reconstruct the seasonal cycle of sea surface temperature (SST) at Henderson Island, southeast Pacific (24°S, 128°W) during the Marine Isotope Stage (MIS) 9 interglacial (~ 339–303 ka). Previously-published closed-system U-series ages provide broad age constraints for the timing of reef growth for this unit on Henderson Island, ranging between 334 and 306 ka. We apply published $\delta^{18}O$-SST slope relationships to the stacked $\delta^{18}O$ annual cycle in the fossil *Porites*, and find the amplitude of the seasonal cycle of SST recorded by the MIS 9 coral to be ~ 4.1 ± 0.57°C, which agrees within error with the modern seasonal cycle of SST (~ 4.1°C). Sr/Ca-SST slope relationships applied to the fossil *Porites* stacked Sr/Ca annual cycle suggest the amplitude of the seasonal cycle of SST was ~ 4.7 ± 0.75°C, exceeding the modern cycle by ~ 15%, but within error of the modern value. Taken together, these results suggest the seasonal cycle of SST at Henderson Island during MIS 9 equaled or exceeded the modern amplitude. Using modern latitudinal relationships between insolation seasonality and SST seasonality, we present a new application for SST amplitudes reconstructed from fossil corals that can be used in conjunction with U-series ages to provide additional geochronological constraints on the development of open-ocean, interglacial reefs.

Keywords: fossil coral; SST; $\delta^{18}O$; Sr/Ca; U/Ca; seasonality; insolation forcing; southeast Pacific

1. Introduction

Seasonality is an inherent feature of climate systems, and has played a major role in the evolution of Earth's climate [1]. Past changes in insolation received during the austral summer at latitude 65°N are central to climate change theory in that they are believed to drive the growth and decay of the massive Northern Hemisphere ice sheets (the Milankovitch theory of climate change) [2,3]. More recently, it has been proposed that large increases in seasonal temperature contrasts over continental Europe and Greenland due to severe winter cooling, are linked to abrupt climate switches in the Northern Hemisphere, such as the Younger Dryas and Heinrich events [4]. Enhanced seasonal changes in

* Corresponding author. Now at: Geoscience Australia, GPO Box 378, Canberra, ACT 2601, Australia. Tel.: +61 2 6249 9111; fax: +61 2 6249 9999.
E-mail address: Bridget.Ayling@ga.gov.au (B.F. Ayling).

0012-821X/$ - see front matter © 2006 Elsevier B.V. All rights reserved.
doi:10.1016/j.epsl.2006.06.009

temperature during these cold events appears to correlate with the altered behavior of major climate systems such as the Indian and East-Asian summer monsoons, which were weaker during these times [5,6]. In contrast, modeling studies suggest that during the mid-Holocene, Northern Hemisphere monsoons were enhanced in response to increases in the amplitude of the seasonal cycle of solar radiation (hereafter 'insolation seasonality') due to orbital forcing [7].

Combining the use of geochemical climate proxies in fast-growing climate archives such as mollusks or tropical corals, with high resolution analytical sampling techniques, allows seasonal and sub-seasonal processes to be resolved, including discrete events such as floods and phytoplankton blooms, and seasonal phenomena such as upwelling and rainfall [8–13]. Importantly, these high-resolution proxy records can provide detailed information on the amplitude and characteristics of the seasonal cycle of a given variable (rainfall, sea surface temperature (SST) etc).

Sr/Ca and oxygen isotope ratios ($\delta^{18}O$) in the skeletons of massive, long-lived hermatypic corals (in particular *Porites* sp.) are excellent recorders of the seasonal cycle of SST in the past. Depending on climatic setting, $\delta^{18}O$ can reflect SST [14,15], sea surface salinity (SSS) [16–18], or a composite signal of SST and SSS [19,20]. In contrast, Sr/Ca ratios in corals are mainly dependent on temperature [10,21–23], although over interglacial/glacial (IG/G) timescales the possibility of variations in the seawater Sr/Ca ratio cannot be excluded [24,25]. Application of these geochemical relationships to fossil *Porites* from the last 130 thousand years (kyr) has enabled reconstruction of climatic conditions during the last IG/G cycle and also during the Penultimate Deglaciation [26–31]. However, high resolution coral records for previous time periods are limited to two other studies [32,33].

Here we use these geochemical proxies in a fossil *Porites* coral to reconstruct the seasonal cycle of SST at Henderson Island, southeast Pacific, during the Marine Isotope Stage (MIS) 9 interglacial ~ 339–303 thousand years ago (ka). Our seasonally resolved coral record from Henderson Island is the first reported for an interglacial period predating MIS 7, and one of the few interglacial records from the Southern Hemisphere; the majority of interglacial coral records are limited to the Northern Hemisphere, from MIS 5.5 and the Holocene [29–31,34,35]. The MIS 9 interglacial is interesting as it appears to have had the highest natural concentrations of atmospheric CO_2 and CH_4 for the last 500 kyr [36]. Moreover, ice core deuterium records [36] and natural gamma ray emission records from Chatham Rise sediments off the east coast of New Zealand [37] both suggest the warmest temperatures over Antarctica for the last 500 kyr were experienced during MIS 9. The SPECMAP stacked planktonic foraminiferal $\delta^{18}O$ record from multiple deep sea cores suggests that MIS 9 has a single dominant peak at 330 ka (MIS 9.3), with a secondary peak at 310 ka (MIS 9.1) [3]. Closed-system coral U-series disequilibrium ages suggest that sea level peaked at 324±3 ka and high sea levels were sustained until 318±3 ka, slightly lagging the peak in summer insolation at 65°N that occurred at 333 ka [38].

2. Physiography and climatic setting of Henderson Island

Henderson Island is part of the Pitcairn Island Group (23–26°S, 122–130°W), which also includes Pitcairn Island (a volcanic island), Oeno Atoll and Ducie Atoll. These islands lie in the extreme east of the Indo-Pacific subtropical province and are isolated from their nearest neighbors (1000 km east, 450 km west) and, in a Pacific Ocean basin context, from New Zealand and South America (>4500 km away, Fig. 1A). Henderson Island is at the environmental limit of coral reef growth, in terms of SST and species biodiversity [39,40], hence it is believed to be a sensitive site from which to monitor changes in past climate.

Henderson Island is an uplifted Pleistocene atoll, with a central paleo-lagoon surrounded by a raised reef structure which displays spur and groove topography [41,42]. The flat-topped surface of the island displays karren features, and is vegetated by thick *Pisonia* scrub. The fossil atoll is approximately 30 m above mean sea level (MSL) and is surrounded by steep cliffs on most sides of the island. Erosion is enhanced on the eastern side of the island due to the prevailing southeast trade winds, and the modern coral reef at Henderson Island is depauperate owing to low species diversity and local bio-erosion processes [40].

Initial fossil coral samples were collected from Henderson Island from several reef transects during the 1991 Sir-Peter Scott Commemorative Expedition to the Pitcairn Islands [42], and later dated by U-series using both TIMS (RSES, ANU) and MC-ICPMS (University of Michigan). Results indicate two main phases of reef growth on Henderson Island: a major atoll construction phase during MIS 15 (~ 630±21 ka), and the development of a fringing reef during MIS 9 [38] (Fig. 1C). Closed-system U-series ages from the fringing reef unit range between 334 ka and 306 ka. The two end-member scenarios consistent with these ages suggest they either reflect several discrete episodes

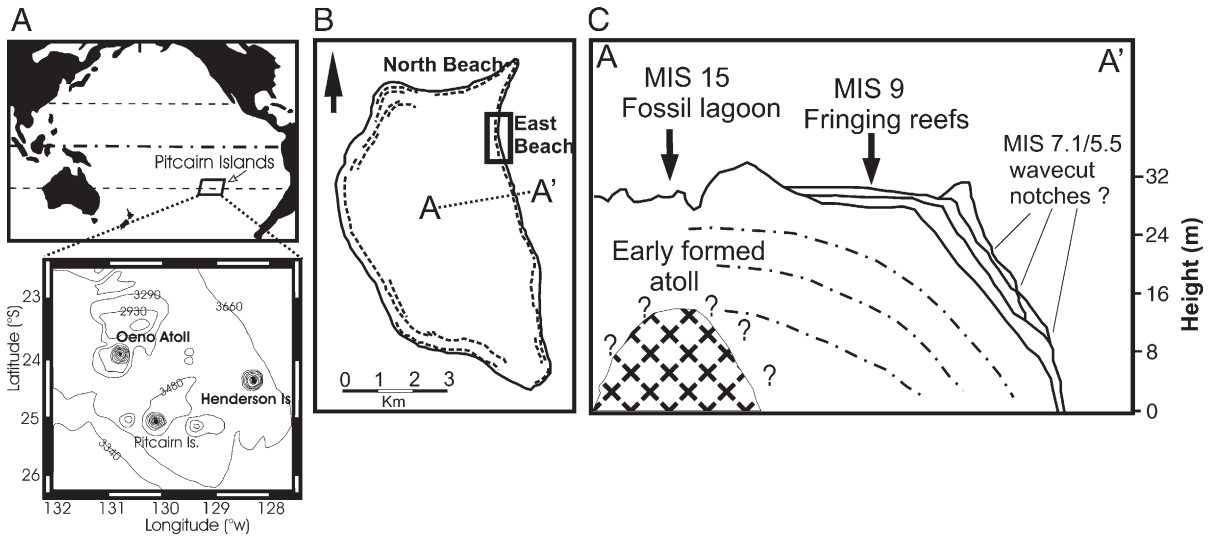

Fig. 1. Geographic setting of Henderson Island and Oeno Atoll. (A) Location of Henderson Island and Oeno Atoll in the Pitcairn Island Group. (B) Location of fossil coral sample sites (box) on East Beach, Henderson Island. (C) Schematic cross section of raised coral reefs on Henderson Island (modified from Stirling et al. [38]), with position of the fossil *Porites* coral analyzed in this study marked.

of reef growth separated by periods of lower sea level or an extremely long interglacial with continuous reef growth on Henderson Island [38]. The true reef growth curve probably lies somewhere in between these two extremes [38]. Based on the stratigraphy of the fringing reef, these reef building episodes were tentatively correlated with interstadials MIS 9.3 and 9.1, where MIS 9.3 is represented by massive reef complexes developed during a prolonged period of stable sea level and smaller corals draping over this unit represent the later MIS 9.1 interstadial.

The sample analyzed in this study was collected during another expedition to Henderson Island in February–March 2003, which amongst other purposes, targeted well-preserved fossil *Porites* specimens for paleoclimatology. Fossil *Porites* specimens from the East Beach cliff sections were found to be in better condition than those from North Beach, and the *Porites* sample analyzed in this study was collected from a massive, extensive paleoreef on the eastern coastline of Henderson Island (East Beach), which consisted of *Porites* and *Faviidae* coral species (see Fig. 1B). U-series dates from this *Porites* coral did not produce reliable age estimates as this paleo-reef has experienced higher levels of U–Th mobilization compared with other reef localities on Henderson Island. Furthermore, *Porites* are usually more susceptible to alteration than thicker walled species. However recently obtained U-series ages from several adjacent *Faviidae* corals in the reef unit suggests that it belongs to MIS 9 although the *Faviidae* corals fail the screening criteria for acceptable dates (Table 1). Open system model ages based on a model in which extraneous ^{234}U and ^{230}Th are added continuously to the coral skeleton through processes of α-recoil (Thompson et al. [43]), suggest that the coral unit may belong to the younger MIS 9.1 period (~ 300±15 ka). However the

Table 1
U-series ages for Henderson Island corals

Sample [a]	$(^{234}U/^{238}U)_{act}$ [b]	$(^{230}Th/^{238}U)_{act}$ [b]	Age (ka) [b]	$(^{234}U/^{238}U)_i$ [c]	O–S age (ka) [d]
NEB 2	1.0735±3	1.0498±4	340.5±1.2	1.1925±11	308±7
NEB 4	1.0803±3	1.0550±5	333.6±1.2	1.2061±11	293±8
NEB 5	1.0871±3	1.0818±5	374.4±1.8	1.2570±15	307±5

Measurements were conducted at the ETH, Zürich and methods and measurement protocols are described in [45,46]. Further technique descriptions are in preparation. All errors are $2\sigma_M$ and refer to the last significant figures associated with the measurements.

[a] Samples are wall fractions of *Faviidae* corals belonging to the same reef unit as the fossil *Porites* coral for which SST data are reported.

[b] Measured relative to Harwell Uraninite HU-1 assuming secular equilibrium with respect to ^{238}U, ^{234}U and ^{230}Th and using half-lives from Cheng et al. [47]. Age uncertainties exclude the contribution from the decay constants.

[c] Back-calculated initial $^{234}U/^{238}U$.

[d] "Open system" (O–S) ages are obtained using the open-system model described in Thompson et al. [43].

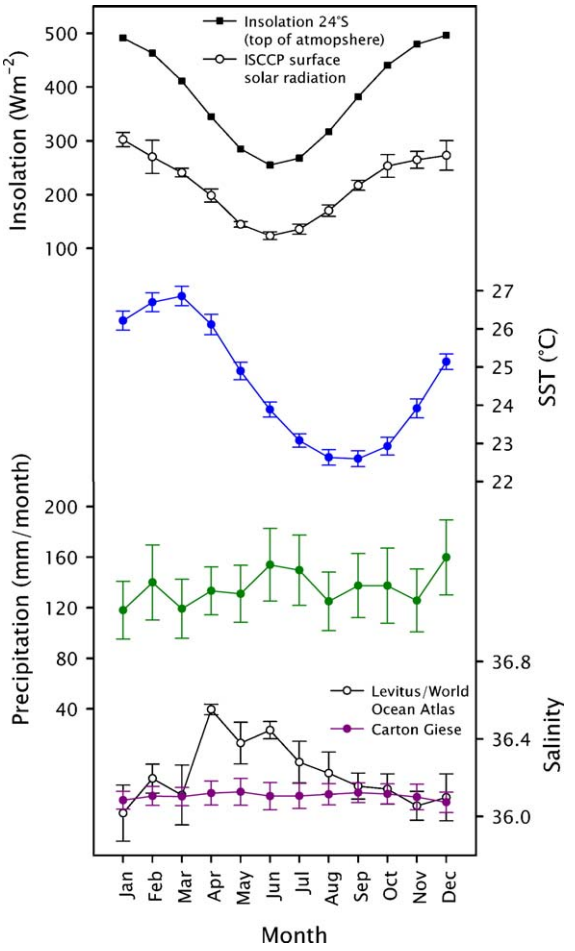

Fig. 2. Relationship between monthly climatologies of solar radiation, SST, salinity and precipitation at Henderson Island. Error bars represent 95% confidence limits for individual data points. Data sources: Top of atmosphere insolation calculated using Analyseries software [78]. Monthly surface solar radiation data (1983–1990) from the International Satellite Cloud Climatology Project: http://iridl.ldeo.columbia.edu/SOURCES/.ISCCP/.derived/.srb/. Monthly SST data (Jan 1982–May 2004) from http://iridl.ldeo.columbia.edu/SOURCES/.NOAA/.NCEP/.EMC/.CMB/.GLOBAL/.Reyn_SmithOIv2/.monthly/.sst/. Monthly precipitation data from combined satellite-gauge measurements from the Global Precipitation Climatology Project (Jan 1987–Jan 2004): http://iridl.ldeo.columbia.edu/SOURCES/.NASA/.GPCP/.V2/.TOVS/.prcp/. Monthly salinity data from Levitus 1994 and the World Ocean Atlas 1998 and 2001: http://iridl.ldeo.columbia.edu/SOURCES/.LEVITUS94/.MONTHLY/.sal/. http://iridl.ldeo.columbia.edu/SOURCES/.NOAA/.NODC/.WOA98/.

accuracy and the application range of the "open system age" model of Thompson et al. [43] is still contentious and not always applicable, and hence we tentatively correlate this reef unit to MIS 9.1. It is possible for example, that open-system models overcorrect the U-series ages to anomalously young values due to additional diagenetic processes that are not accounted for. Further U-series and diagenesis work is in preparation to reconcile the U-series ages for the fossil *Porites* paleo-reef unit with those for other sampling localities on Henderson Island [44].

Oceanographically, the Pitcairn Island Group is situated near the center of the South Pacific gyre, removed from the equatorial Pacific zonal SST gradient and associated Walker circulation, and also the South Pacific Convergence Zone. As such, this subtropical site is not strongly influenced by interannual SST anomalies associated with the El Niño Southern Oscillation (ENSO). Rainfall and SSS both display weak seasonality, indicating good potential for $\delta^{18}O$ thermometry at this site. Henderson Island is located near the center of an area of relatively high sea surface salinity in the Pacific (>36) [48], which is associated with the arid conditions that prevail within the South Pacific gyre. Surface insolation reaches a maximum in January and maximum SSTs occur in March, lagging the solar radiation maxima by 2 months due to oceanic thermal inertia (Fig. 2).

3. Methods

3.1. Coral sampling

The modern coral reef at Henderson Island is depauperate, and no modern *Porites* were located for sampling. Therefore two cores were extracted from a modern *Porites* sp. colony living in 5 m water depth in the lagoon at Oeno Atoll, located ~ 200 km northwest of Henderson Island. Although the lagoonal environment of Oeno Atoll is not a good analogy for the open-ocean, fringing-reef that characterizes Henderson Island, it is useful for providing constraints on the extent of *in-situ* diagenetic alteration in the fossil *Porites* samples. Fossil coral samples from the MIS 9 reef at Henderson Island were collected in February 2003 using a paleo-magnetic drill, or hammer and chisel, at elevations between 4 m and 30 m above MSL. The sample analyzed for this study was collected (using hammer and chisel) from a large (~ 3 m) fossil *Porites* colony located ~ 6 m above MSL (GPS location: 24°20.551′S, 128°18.110′W). No field observations could provide any constraints on the growth period of this reef unit (e.g. MIS 9.3 or 9.1).

3.2. Assessment of diagenetic alteration

The fossil *Porites* specimen used for this study was identified as the most pristine of multiple samples collected from Henderson Island, and therefore best suited for paleoclimatology. Samples were screened for diagenetic alteration using X-ray diffraction (XRD) analysis (to detect calcite), petrographic thin sections

(to detect pore infilling or skeletal recrystallization), and scanning electron microscopy (SEM), which allow crystal character and areas affected by dissolution to be identified.

3.3. Coral cleaning and microsampling

8 mm-coral slabs were created from our sample and X-rayed to identify major growth axes for microsampling (Fig. 3). Prior to microsampling, the 8 mm slabs were vigorously cleaned in Milli-Q water beneath an ultrasonic probe to remove surface contaminants, salt trapped in pores and secondary aragonite needles (which could be crucial for obtaining good Sr/Ca data from fossil corals) [49]. Coral samples were milled every 0.25 mm, which corresponds to approximately weekly resolution, given that the fossil coral had an average extension rate of ~ 11 mm/yr. The 2 mm × 2 mm cross-sectional area of each micro-sample is designed specifically to ensure equal representation of skeletal elements in each sample, thus avoiding day vs. night calcification within a single coral calyx [49]. This is particularly important for Sr/Ca because it minimizes fine-scale "biological noise" and enhances the temperature signal.

3.4. Stable isotope measurements

Every fourth sample from the transect was analyzed for $\delta^{18}O$ and $\delta^{13}C$ in an automated Kiel carbonate preparation device coupled to the inlet system of a Finnigan MAT-251 mass spectrometer at the RSES, ANU. Coral powders weighing between 190 and 220 μg were reacted with 2 drops of 103% H_3PO_4 at 90°C. Water was removed from the evolved H_2O–CO_2 gas from this reaction by freezing and then vaporizing CO_2 in a double trap system using liquid nitrogen. The pure CO_2 gas then enters the inlet system of the mass spectrometer for measurement. All isotopic data are reported as per mil (‰) deviations relative to the Vienna Peedee Belemnite standard (VPDB), based on measurements of National Bureau of Standards NBS-19 ($\delta^{18}O = -2.20$‰). Analytical precision for replicate measurements ($n = 125$) of $\delta^{18}O$ in NBS-19 was ±0.09‰ (2SD).

3.5. Sr/Ca measurements (thermal ionization mass spectrometry)

Coral carbonate samples weighing between 80 and 150 μg were dissolved, from which 5–10 μg aliquots were analyzed using isotope dilution thermal ionization mass spectrometry (ID-TIMS) on a MAT 261 mass spectrometer at the RSES, ANU following the methods described by Alibert and McCulloch [22] and Marshall and McCulloch [23]. Each Sr/Ca sub-sample was taken from the same samples on which stable isotope measurements were performed. Analytical precision for replicate measurements ($n = 16$) of Sr/Ca in an in-house laboratory standard was ±0.02 mmol mol^{-1} (2 S.D.).

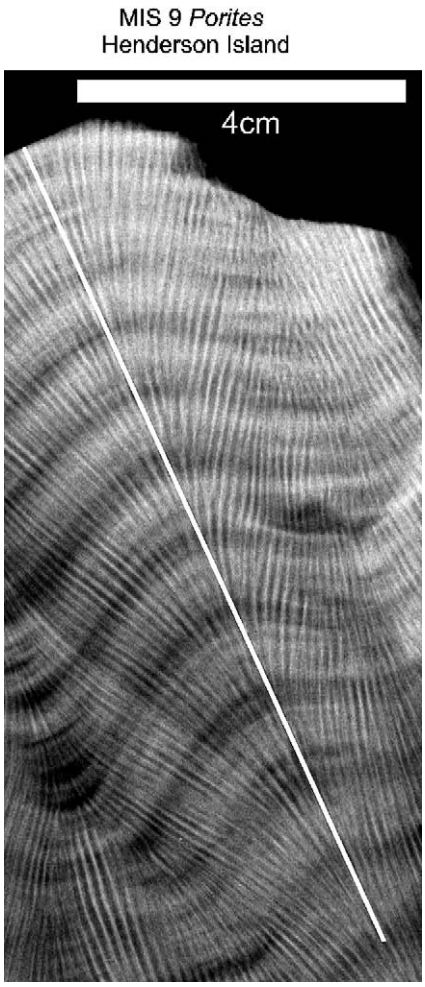

Fig. 3. X-ray positive image of the MIS 9 fossil *Porites* coral from Henderson Island. Couplets of high skeletal density (dark bands) and low skeletal density (light bands) represent one annual growth increment. Sampling transect for stable isotope and Sr/Ca analyses is indicated by thick white line.

3.6. Laser ablation inductively coupled plasma mass spectrometry (LA-ICPMS)

Coral segments not exceeding 20 mm in diameter and 90 mm in length were analyzed for Sr/Ca and U/Ca composition on a Quadrupole PQ2 inductively coupled plasma mass spectrometer connected to a laser ablation sampling cell at the RSES, ANU, following methods

described by Sinclair [50] and Fallon et al. [51]. Samples were ablated using an ArF excimer laser (193 nm wavelength) pulsed at 5 Hz with an energy density of 50 mJ, and masked to produce a beam 500 μm long in the direction perpendicular to the growth axis and 50 μm wide parallel to the growth axis. Based on analysis of the ANU Davies Reef coral standard in a pressed-powder disc, analytical precision of the LA-ICPMS technique expressed as relative standard deviation was ±1.2% for Sr/Ca and ±3.4% for U/Ca.

3.7. Sr/Ca and $\delta^{18}O$ thermometry

To reconstruct MIS 9 SSTs at Henderson Island, a representative modern SST calibration is needed; ideally this should be generated from a living *Porites* at Henderson Island. As the modern reef at Henderson Island is poorly developed, no living *Porites* colonies were found, and therefore a modern *Porites* colony was sampled from the lagoon at Oeno Atoll (~ 200 km north-west of Henderson Island). However SST calibration equations developed from this specimen suggest that lagoonal processes (such as heating and/or evaporation) are modulating the seasonal cycle of SST. Calibrating these proxies for *Porites* in this lagoonal environment against IGOSS open-ocean SST produced low-slope calibrations that cannot be applied to fringing-reef fossil corals. Thus average-slope values were calculated from previously published $\delta^{18}O$-SST and Sr/Ca-SST relationships for *Porites* corals from the wider Indo-Pacific region (Table 2). Average slope values of 0.065 mmol mol^{-1}/°C for Sr/Ca, and −0.166‰/°C for $\delta^{18}O$ were calculated from eight and six reef settings respectively, and provide a sound basis for reconstructing MIS 9 SST seasonality at Henderson Island. The errors associated with these slopes are taken

Table 2
Sr/Ca-SST and $\delta^{18}O$-SST calibration equations for *Porites* of the Indo-Pacific region

Equation	Ref.	Location	Lat.	Slope average (‰/°C)	Reconstructed SST at $\delta^{18}O$=−3.30‰
$\delta^{18}O=-1.21-0.134\times SST$	[52]	Ryukyu Islands, Japan	29°N		15.6
$\delta^{18}O=-0.611-0.165\times SST$	[53]	Ryukyu Islands, Japan	29°N	−0.15	16.3
$\delta^{18}O=-0.86-0.150\times SST$	[54]	Guam, NW Pacific	13°N		16.3
$\delta^{18}O=-1.09-0.140\times SST$	[54]	Guam, NW Pacific	13°N	−0.15	15.8
$\delta^{18}O=-0.026-0.196\times SST$	[55]	Panama	8°N	−0.196	16.7
$\delta^{18}O=-1.02-0.174\times SST$	[56]	S. China Sea	20°N	−0.17	13.1
$\delta^{18}O=0.002-0.174\times SST$	[20]	Orpheus Is. GBR	19°S		19.0
$\delta^{18}O=0.447-0.189\times SST$	[20]	Orpheus Is. GBR	19°S		19.8
$\delta^{18}O=0.183-0.180\times SST$	[57]	Pandora Reef, GBR	19°S	−0.18	19.4
$\delta^{18}O=1.23-0.133\times SST$	[58]	New Caledonia	22°S		34.1
$\delta^{18}O=-0.91-0.151\times SST$	[59]	New Caledonia	22°S		15.8
$\delta^{18}O=0.004-0.189\times SST$	[60]	New Caledonia	22°S	−0.16	17.5
Average $\delta^{18}O$ slope (‰/°C)=−0.166					

Equation	Ref.	Location	Lat.	Slope avg (mmol mol^{-1}/°C)	Reconstructed SST at Sr/Ca=9.35 (mmol mol^{-1})
$Sr/Ca\times10^3=10.76-0.063\times SST$	[51]	Shirigai Bay, Japan	32°N	−0.063	22.4
$Sr/Ca\times10^3=10.956-0.079\times SST$	[61]	Hawaii	21°N	−0.079	20.3
$Sr/Ca\times10^3=10.286-0.0514\times SST$	[62]	Taiwan	22°N		18.2
$Sr/Ca\times10^3=9.836-0.0424\times SST$	[56]	S. China Sea	20°N	−0.0469	11.5
$Sr/Ca\times10^3=11.57-0.0823\times SST$	[63]	Rarotonga	22°S	−0.0823	27.0
$Sr/Ca\times10^3=10.48-0.0615\times SST$	[22]	Davies Reef, GBR	19°S		18.4
$Sr/Ca\times10^3=10.40-0.0575\times SST$	[34]	Myrmidon Reef, GBR	19°S		18.3
$Sr/Ca\times10^3=10.73-0.0639\times SST$	[20]	Orpheus Is, GBR	19°S	−0.061	21.6
$Sr/Ca\times10^3=10.78-0.066\times SST$	[20]	Java, Indonesia	8°S		21.7
$Sr/Ca\times10^3=10.51-0.062\times SST$	[64]	Alor, Indonesia	8°S	−0.064	18.7
$Sr/Ca\times10^3=10.68-0.0616\times SST$	[20]	Indian Ocean	20°S		21.6
$Sr/Ca\times10^3=10.375-0.0593\times SST$	[65]	Indian Ocean	10°S	−0.0605	17.3
$Sr/Ca\times10^3=10.479-0.06245\times SST$	[66]	New Caledonia	22°S		18.1
$Sr/Ca\times10^3=10.073-0.052\times SST$	[67]	New Caledonia	22°S		13.9
$Sr/Ca\times10^3=10.73-0.06567\times SST$	[68]	New Caledonia	22°S		21.0
$Sr/Ca\times10^3=10.51-0.062\times SST$	[64]	New Caledonia	22°S	−0.0605	18.7
Average Sr/Ca slope (mmol mol^{-1}/°C)=−0.065					

as 2 SE of the mean slope value, equal to 0.008 mmol mol^{-1}/°C and 0.016‰/°C respectively.

4. Results

4.1. Coral preservation

The fossil corals of Henderson Island are exceptionally well preserved for corals of MIS 9 age, which likely reflects the arid environment and limited meteoric water circulation on Henderson Island. XRD analysis indicates the sample analyzed in this study was 100±1% aragonite (the uncertainty in XRD is ~ 1%). The main feature observed in the MIS 9 *Porites* is dissolution of the centers of calcification (COC) (sometimes also known as early mineralization zones (EMZ)) (Fig. 4). In both the modern and fossil *Porites*, these centers of calcification appear as brown areas in thin section (Fig. 4A,B) because the submicron size of these crystals alters how light is transmitted [69]. Dissolution pits in the COC are visible in both modern and fossil samples under a SEM, in both Scanning Electron (SE) or Backscattered Electron (BSE) mode (see Fig. 4E,F). This preferential dissolution of skeletal aragonite is consistent with previous findings, where is has been suggested that the small crystal size of calcification centers in addition to their poor crystallization (random crystal orientation) increases their chemical reactivity [69,70]. In addition, greater amounts of organic matrix are present in the EMZ relative to the fibrous aragonite zones, specifically acidic polysaccharides and organic acidic chondroitin sulfate, which may play an important role in their preferential dissolution [71].

4.2. Fossil coral geochemistry

The geochemical records for the MIS 9 coral are displayed in Fig. 5. Strong seasonality is preserved in the fossil *Porites* Sr/Ca and $\delta^{18}O$, which vary about mean values of ~ 9.35 mmol mol^{-1} (TIMS) and −3.30‰ respectively. Sr/Ca data acquired from the same growth axis using LA-ICPMS techniques displays good agreement with the TIMS Sr/Ca data, with a mean Sr/Ca value of 9.30 mmol mol^{-1}, although the precision of LA-ICPMS Sr/Ca is lower (~ 1.2% relative standard deviation vs. ~ 0.2% for TIMS). U/Ca varies about a mean value of 1.2 μmol/mol and displays strong seasonality, suggesting uranium incorporation in this

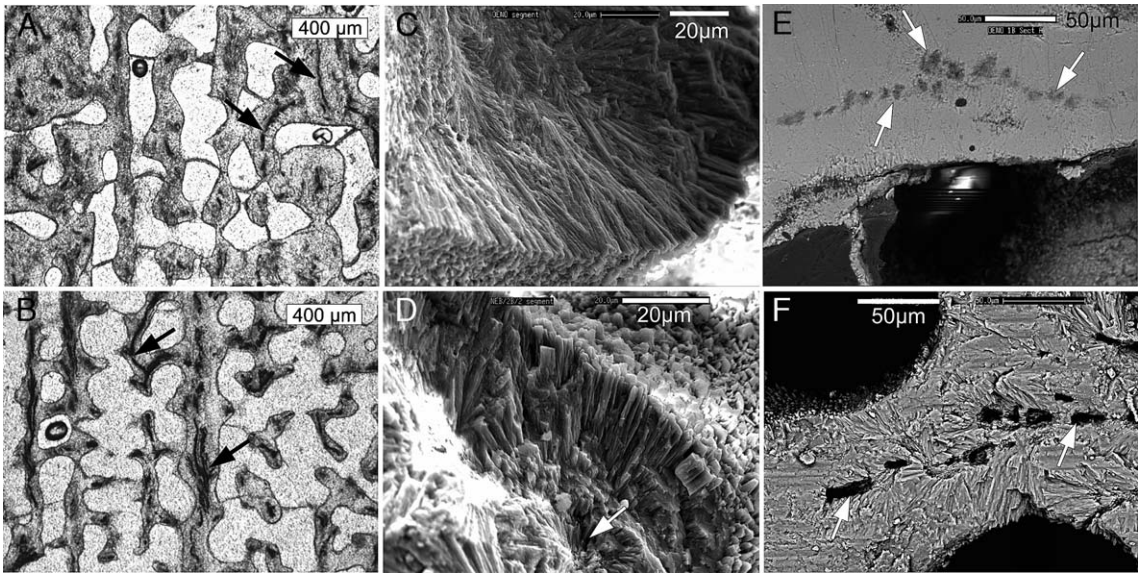

Fig. 4. Comparison of skeletal aragonite in the modern and fossil *Porites* corals. (A) Photomicrograph of a petrographic thin section of the modern *Porites* from Oeno Atoll in plane polarized light. Skeletal walls and calcification centers (arrows) are easily identified. (B) Thin-section photomicrograph of fossil *Porites* from Henderson Island. Excellent preservation of primary porosity is evident, and no calcite in-fills or secondary aragonite are visible. Arrows indicate calcification centers, which appear wider than those in the modern *Porites* specimen. (C) Scanning electron (SE) image of the modern *Porites*. Primary aragonite fibers are clear and form a fan around a calcification center. (D) SE image of the fossil *Porites.* Slight dissolution of a calcification center is indicated by the 'pitted' appearance (arrow), however surrounding aragonite fibers appear pristine. (E) High magnification SE image of the modern *Porites*. Grey patches indicated by arrows reflect voids where calcification centers have experienced incipient dissolution. (F) Backscattered electron (BSE) image of the fossil *Porites* illustrating advanced dissolution of calcification centers (indicated by arrows).

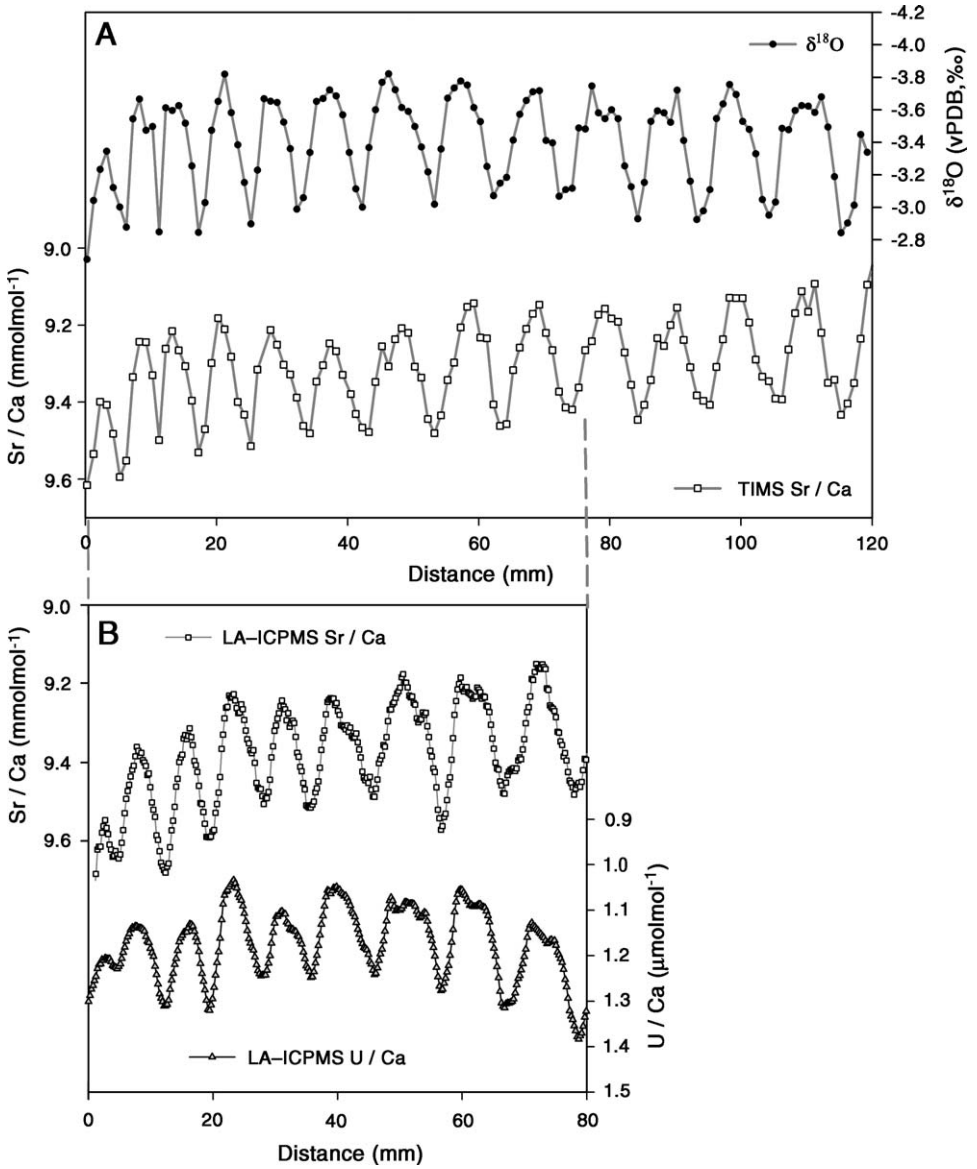

Fig. 5. Plots of skeletal Sr/Ca and $\delta^{18}O$ for the MIS 9 fossil *Porites*. (A) Fossil *Porites* $\delta^{18}O$ and TIMS Sr/Ca record. Samples were analyzed at 1 mm intervals along the microsampling transect to give approximate monthly resolution. (B) Sr/Ca and U/Ca record measured on a parallel growth axis using LA-ICPMS. Good agreement is observed between Sr/Ca measured using the TIMS and LA-ICPMS techniques.

fossil *Porites* was influenced by SST. In coral proxy records, the presence of annual cycles in proxies such as Sr/Ca or $\delta^{18}O$ is generally inferred to support good sample preservation. Given that the petrographic observations suggest minimal diagenetic alteration of this fossil coral, and distinct annual cycles are observed in fossil coral Sr/Ca and $\delta^{18}O$, this MIS 9 coral appears to be very well preserved. Moreover, LA-ICPMS measurements indicate clear annual cycles in the fossil *Porites* U/Ca, which has been suggested to indicate primary aragonite [72,73].

4.3. SST seasonality during MIS 9

Reconstructing absolute temperatures over interglacial/glacial timescales using modern proxy-SST calibration equations can be problematic. For the Sr/Ca proxy, corals from the same location display a wide range in reconstructed SST for the same Sr/Ca value (11–27 °C for the MIS 9 fossil coral mean Sr/Ca of 9.35 mmol mol^{-1}) (Table 2). Even for corals in the same geographic region, large differences exist (between 3 and 7 °C) in the SSTs that are reconstructed using their Sr/Ca-SST calibrations. This

range in reconstructed temperatures stems from differences in absolute Sr/Ca values between individual colonies, which may reflect slight differences in their Sr distribution coefficients (D_{Sr}=(Sr/Ca)$_{aragonite}$/(Sr/Ca)$_{seawater}$) owing to possible biological influences [74–77]. Thus even assuming that factors such as changes in seawater Sr/Ca ratio are not occurring over interglacial/glacial timescales [24,25], we still cannot be certain that a modern *Porites* Sr/Ca-SST calibration from Henderson Island would be applicable to a MIS 9 *Porites* from Henderson Island. Reconstruction of absolute temperatures using the δ^{18}O proxy is also complicated, owing to potential changes in baseline salinity values (large-scale, ocean basin changes), poorly constrained ice volume contributions, and biological effects.

Considering these uncertainties, the best approach remains to apply the average-slope relationships to the fossil coral data to obtain estimates of the amplitude of the seasonal cycle of SST during MIS 9. After applying the average-slope relationships described earlier (Table 2), the instrumental and coral records were re-sampled at monthly resolution using Analyseries software [78] and stacked. These stacked records are compared with the modern seasonal cycle of IGOSS SST for the 1°×1° grid that surrounds Henderson Island (Fig. 6).

The average amplitude of the modern SST cycle at Henderson Island is approximately 4.1 °C (the mean value for three SST datasets; see Fig. 6 for data sources). The fossil coral δ^{18}O record indicates that the seasonal cycle of SST during MIS 9 at Henderson Island was also 4.1 °C (±0.57 °C, 2 SE), which is statistically indistinguishable from SST seasonality in the modern oceanic setting at Henderson Island. A slightly larger seasonal cycle (4.7±0.75 °C, 2 SE) is indicated by the fossil coral Sr/Ca, which suggests a ~ 15% (±18%) increase in SST seasonality. The errors for these estimates include the uncertainty associated with the average Sr/Ca-SST or δ^{18}O-SST slope relationship (a 'gradient error', taken as 2 SE of the mean), and the uncertainty associated with the reproducibility of the mean value for each data-point in the average annual cycle (also 2 SE); these values were added in quadrature. The overall error for each data-point could be reduced if more annual cycles are stacked to reduce the uncertainty associated with each data-point (only 13 yrs were analyzed in this fossil *Porites*). The 'gradient error' could potentially be reduced if proxy-SST calibrations were generated from multiple modern *Porites* corals from the same location where fossil *Porites* are sampled, which was not possible in this study. We have conservatively included corals from a broad geographic distribution, and all may not be representative of mid-oceanic corals. In summary, the results suggest that SST seasonality at Henderson Island during this period of MIS 9 was similar to, or slightly greater than, the amplitude of the modern seasonal cycle.

5. Discussion

5.1. Implications for fossil coral SST seasonality

Although our findings suggest that the seasonal cycle of SST during MIS 9 was within error of the modern SST

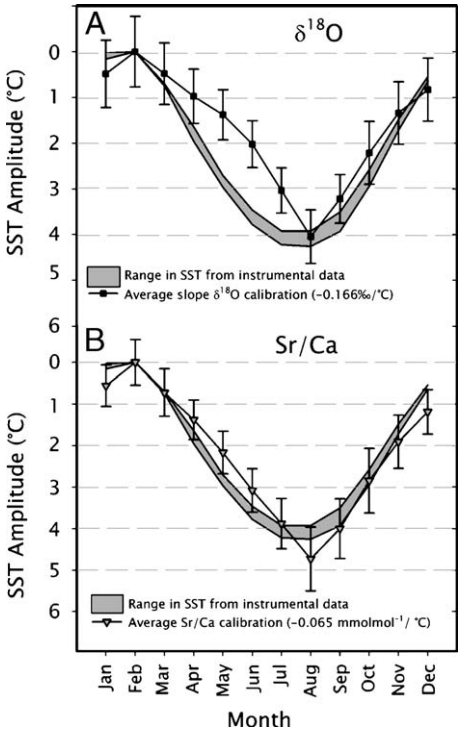

Fig. 6. Amplitudes of average annual cycles of SST reconstructed from fossil coral δ^{18}O and Sr/Ca relative to modern annual SST cycle. (A) Comparison of composite monthly record of MIS 9 SST reconstructed from coral δ^{18}O and the modern instrumental record of SST. (B) Comparison of composite monthly record of MIS 9 SST reconstructed from coral Sr/Ca and the modern instrumental record of SST. The average δ^{18}O-SST and Sr/Ca-SST slope relationships in Table 2 have been used for the reconstructions. Records for MIS 9 have been normalized to February of the modern record in order to display the difference in amplitude for each proxy. Vertical bars show 2 SE limits for individual data points in the coral records, which includes the error associated with the reproducibility of each data point, and the error in the average-slope value estimate. The amplitudes of the δ^{18}O and Sr/Ca composites for MIS 9 equal, or exceed (0–15%), modern amplitudes (2SE). Range of modern SST cycle at Henderson Island sourced from three datasets: http://iridl.ldeo.columbia.edu/SOURCES/.NOAA/.NCEP/.EMC/.CMB/.GLOBAL/.Reyn_SmithOIv2/.monthly/.sst/. http://iridl.ldeo.columbia.edu/SOURCES/.NOAA/.NCEP/.EMC/.CMB/.Pacific/.monthly/.temp/. http://iridl.ldeo.columbia.edu/SOURCES/.NOAA/.NCDC/.ERSST/.version2/.SST/.

cycle, given appropriate average-slope calibrations, it may be possible to utilize amplitudes of the seasonal cycles of SST in the past to provide geochronological constraints on the timing of coral reef growth.

In the modern ocean, the amplitude of the seasonal cycle of SST in the tropics closely follows the seasonal cycle of surface insolation (with a ~ 2 month lag), and away from centers of upwelling, boundary currents and equatorial interannual variability, is largely a function of latitude [79,80]. To illustrate this, we compared the average amplitude of the seasonal cycle of IGOSS SST with insolation seasonality along a north/south transect from Henderson Island, in the subtropics, to the equator (Fig. 7A). A linear relationship is observed between ~ 12°S and ~ 32°S between these two variables, and Henderson Island lies in the center of this 'linear' zone at 25°S. Within 12° of the equator however, the relationship is obscured due to strong seasonal and interannual variability in equatorial upwelling. At subtropical latitudes, the percentage increase in SST and insolation seasonality yields a near 1:1 relationship (Fig. 7B). Given that insolation seasonality in the tropics varies through time due to changes in orbital precession, changes in the amplitudes of the seasonal cycle of SST in the tropics in the past will be diagnostic of different periods within the precession cycle (<21 kyr), which may allow the ages of fossil corals to be constrained at suborbital timescales.

We explore the possibility of using the relationship between insolation and SST to 'fine-tune' the chronology of coral reef growth at Henderson Island during MIS 9. The maximum and minimum insolation seasonalities experienced at Henderson Island during MIS 9 are ~ 11% greater and ~ 34% smaller respectively relative to the modern cycle (Fig. 7C). Using the relationship defined in Fig. 7B, the ~ 15±18% increase in Sr/Ca-reconstructed SST seasonality in the MIS 9 coral should equate to a ~ 12% increase in insolation seasonality, relative to the present. This estimate agrees well with the maximum possible insolation forcing during MIS 9, which is ~ 11% greater than present. Given that SST seasonality recorded by the fossil coral falls between 0% and 15% larger than present, we infer that the insolation seasonality at the time the fossil coral grew equaled or exceeded the modern amplitude.

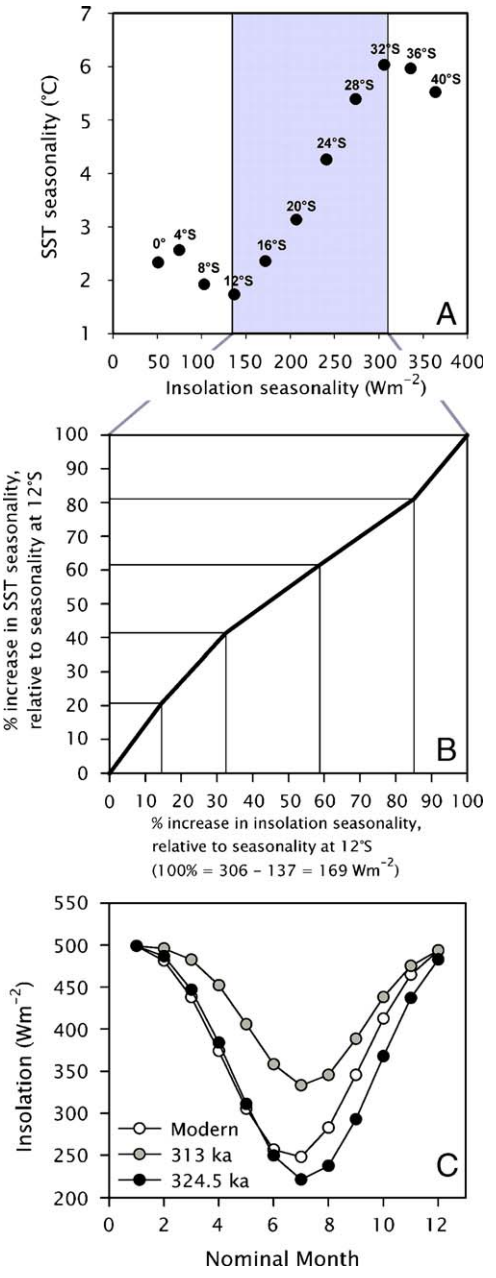

Fig. 7. Latitudinal relationships between amplitudes of annual cycles of SST and insolation (seasonality) at 128°W, 0–40°S. (A) Change in SST seasonality relative to change in insolation seasonality. Within the area covered by the grey box, an approximate linear relationship is observed between these two variables. SST data sourced from http://iridl.ldeo.columbia.edu/SOURCES/.NOAA/.NCEP/.EMC/.CMB/.GLOBAL/.Reyn_SmithOIv2/.monthly/.sst/. Insolation data calculated using Analyseries software [78]. (B) Conversion of this data where a linear relationship is observed, to relative percentage increase, reveals a near 1:1 covariation. (C) Comparison of the modern seasonal cycle of insolation to the minimum and maximum insolation cycles experienced during MIS 9. These records were normalized to the modern January value (498 W/m^2) and shifted so that maximum annual insolation occurred in January (over time, the timing of the seasons change slightly due to the Earth's orbital variations). As we observe SST seasonality that equals or exceeds the modern cycle, we infer our coral must have been growing when the seasonal insolation cycle equaled or exceeded the modern.

Over the last 400 kyr, insolation seasonalities have varied significantly in the northern and southern hemisphere tropics (Fig. 8A). Our results suggest that this particular period of reef growth on Henderson Island correlates to one of two narrow intervals during MIS 9 when insolation seasonality in the southern tropics equaled or exceeded modern values: between 327 and 320 ka (early MIS 9) and again between 306 and 299 ka (late MIS 9) (Fig. 8B). Reliable closed-system U-series ages from Henderson Island suggest peak interglacial conditions of MIS 9 were experienced between 324 and 318 ka [38], whereas open-system U-series ages from this reef unit suggest later reef growth (average age 301 ka, see Table 1). The age-estimates generated using insolation seasonality are thus consistent with both U-series estimates.

5.2. Broad implications

If appropriate average-slope calibrations are applied to fossil corals to reconstruct the seasonal cycle of SST, this new approach could provide insights into the history of global climate change, sea level and coral reef development at suborbital to millennial timescales. Although relatively small increases in insolation seasonality (+10%) were experienced at Henderson Island during the MIS 9 interglacial, much larger increases (+30% to 40%) were experienced in the Northern Hemisphere during the MIS 9 and more recent interglacial periods, such that fossil corals from these intervals are likely to record significant increases in SST seasonality that are statistically different from the modern cycle (Fig. 8A). These large changes are well within the signal recording ability of massive *Porites*. This approach could make it possible to 'fine-tune' coral U-series chronologies within a single precession cycle (21 kyr) by comparing the amplitude of SST recorded by corals. Given reasonable U-series age constraints, the individual coral paleoclimate records could then be placed more accurately within the precession cycle to reveal the nature of abrupt climate change on sub-orbital (millennial) timescales. Importantly, opposing changes in coral records from opposite hemispheres could serve to constrain the precise timing of periods of widespread development of coral reefs, which would signal important turning points in global climate change and eustatic sea level.

Although this technique appears to work well at the mid-oceanic location of Henderson Island, it may be difficult to apply in areas where complex oceanographic/atmospheric interactions occur, such as in equatorial regions where interannual variability in SST is larger than the amplitude of the annual cycle of SST [79], or where boundary currents advect the seasonal thermal signal downstream [80]. Open ocean sites however, should be prime locations to further test this approach.

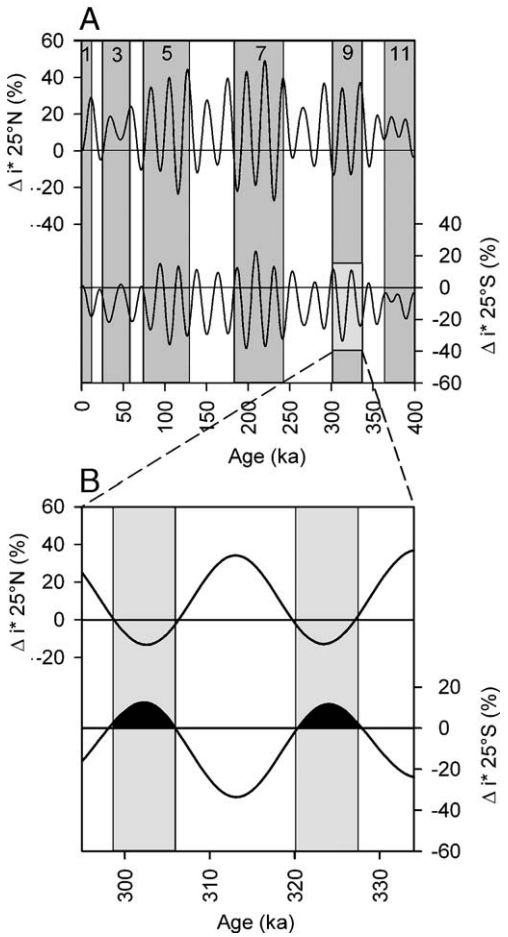

Fig. 8. Insolation seasonality at 25°N and 25°S over the past 400 kyr. (A) Changes in insolation seasonality (December 21st minus June 21st) are calculated as percentage differences relative to modern insolation seasonality (Δi*) at 25°N and 25°S. Box shows timing of MIS 9 (~ 339–303 ka). (B) Close-up of changes in insolation seasonality at 25°N and 25°S during MIS 9. The greater SST seasonality for the MIS 9 coral (reconstructed using δ^{18}O and Sr/Ca) indicates that the coral grew during one of two brief periods of relatively high insolation seasonality (327–320 ka, MIS 9.3 or 306–299 ka, MIS 9.1), when summer insolation in the Northern Hemisphere high latitudes was relatively weak.

6. Conclusions

- Seasonal cycles of Sr/Ca and oxygen isotope ratios (δ^{18}O) can successfully be used in massive fossil *Porites* corals to obtain information about the seasonal cycle in SST. Seasonality is a robust parameter and one of the greatest strengths of fossil coral paleoclimate archives.

Absolute temperatures are more difficult to reconstruct over interglacial/glacial (IG/G) timescales due to uncertainties in ice volume estimates and large scale salinity variations (affecting $\delta^{18}O_{sw}$), and possible IG/G variations in oceanic Sr/Ca, and/or biological effects, which affect coral Sr/Ca SST calibrations.

- Using the average of published coral δ^{18}O-SST and Sr/Ca-SST slope relationships in the Indo-Pacific region, we reconstructed the seasonal cycles of SST for a short interval within MIS 9 (~ 339–303 ka) and found both thermometers to be in close agreement. The seasonal SST cycle reconstructed from fossil coral δ^{18}O is 4.1 °C ± 0.57 °C, agreeing within error with the modern SST cycle (also 4.1 °C). The seasonal cycle of SST reconstructed using coral Sr/Ca indicates an amplitude of 4.7 ± 0.75 °C, which is 15 ± 18% larger than the modern SST cycle.
- In the modern southeastern tropical Pacific Ocean, SST seasonality and insolation seasonality display a near-linear positive correlation between 12°S and 32°S at 128°W. This relationship is close to 1:1, and given reliable reconstructions of SST seasonality in the past, can potentially be used to place constraints on the timing of coral reef growth in the Southern Hemisphere sub-tropics.
- Applying this approach to MIS 9 fossil *Porites* from Henderson Island yields results which are consistent with both closed-system and open-system model U-series ages for coral reef growth on Henderson Island. During MIS 9, insolation seasonality in the southern tropics was often less than at present (reduced by 35%), and only exceeded modern values during two brief intervals between 327–320 ka and 306–299 ka (up to 11% greater at Henderson Island). Given that the MIS 9 fossil coral record suggests the amplitude of the seasonal cycle of SST was equal to or greater (up to 15%) than the modern SST cycle, we infer that the fossil coral grew within the 327–320 ka (peak MIS 9) or 306–299 ka (late MIS 9) intervals.

Acknowledgments

This work was performed under an ARC grant awarded to M.T. McCulloch and an ETH grant awarded to C.H. Stirling, targeting interglacial climates and SL variation. Damien Kelleher, Michael O'Leary and Alve Henricson and the crew of the Research Vessel *Searcher* are gratefully thanked for their significant efforts in making the Henderson Island expedition a success. We thank Graham Mortimer, Lesley Kinsley, Joe Cali and Heather Scott-Gagan for their assistance in performing geochemical analyses. Bill Thompson is thanked for access to his open-system age calculations spreadsheet. Two anonymous reviewers are thanked for their constructive comments, which significantly improved the manuscript. B. Ayling was supported by an ANU PhD Graduate School scholarship.

References

[1] T.J. Crowley, D.A. Short, J.G. Mengel, G.R. North, Role of seasonality in the evolution of climate during the last 100 million years, Science 231 (1985) 579–584.

[2] M.M. Milankovitch, Canon of Insolation and the Ice-age Problem, Königlich Serbische Akademie, Belgrade, Yugoslavia, 1941.

[3] J. Imbrie, J.D. Hays, D.G. Martinson, A. McIntyre, A.C. Mix, J.J. Morley, N.G. Pisias, W.L. Prell, N.J. Shackleton, The orbital theory of Pleistocene climate: Support from a revised chronology of the marine δ^{18}O record, in: A.L. Berger (Ed.), Milankovitch and Climate, Part 1, D. Reidel Publishing Company, Norwell, Mass., 1984, pp. 269–305.

[4] G.H. Denton, R.B. Alley, G.C. Comer, W.S. Broecker, The role of seasonality in abrupt climate change, Quat. Sci. Rev. 24 (2005) 1159–1182.

[5] M.A. Altabet, M.J. Higginson, D.W. Murray, The effect of millennial-scale changes in Arabian Sea denitrification on atmospheric CO_2, Nature 415 (2002) 159–162.

[6] Y.J. Wang, H. Cheng, R.L. Edwards, Z.S. An, J.Y. Wu, C.C. Shen, J.A. Dorale, A high-resolution absolute-dated Late Pleistocene monsoon record from Hulu Cave, China, Science 294 (2001) 2345–2348.

[7] Z. Liu, S.P. Harrison, J. Kutzbach, B. Otto-Bliesner, Global monsoons in the mid-Holocene and oceanic feedback, Clim. Dyn. 22 (2004) 157–182.

[8] R. Takesue, A. van Geen, Mg/Ca, Sr/Ca and stable isotopes in modern and Holocene Protothaca staminea shells from a northern Californian coastal upwelling region, Geochim. Cosmochim. Acta 68 (2004) 3845–3861.

[9] D.L. Lea, G.T. Shen, E.A. Boyle, Coralline barium records temporal variability in equatorial Pacific upwelling, Nature 340 (1989) 373–376.

[10] M.T. McCulloch, M.K. Gagan, G.E. Mortimer, A.R. Chivas, P.J. Isdale, A high-resolution Sr/Ca and δ^{18}O coral record from the Great Barrier Reef, Australia, and the 1982–1983 El-Niño, Geochim. Cosmochim. Acta 58 (1994) 2747–2754.

[11] M.T. McCulloch, S. Fallon, T. Wyndham, E. Hendy, J. Lough, D.J. Barnes, Coral record of increased sediment flux to the inner Great Barrier Reef since European settlement, Nature 421 (2003) 727–730.

[12] M. Morimoto, O. Abe, H. Kayanne, N. Kurita, E. Matsumoto, N. Yoshida, Salinity records for the 1997–98 El Nino from Western Pacific corals, Geophys. Res. Lett. 29 (2002), doi:10.1029/2001GL013521.

[13] E. Vander Putten, F. Dehairs, E. Keppens, W. Baeyens, High resolution distribution of trace elements in the calcite shell later of modern *Mytilus edulis*: environmental and biological controls, Geochim. Cosmochim. Acta 64 (2000) 997–1011.

[14] G.M. Wellington, R.B. Dunbar, G. Merlen, Calibration of stable oxygen isotope signatures in Galapagos corals, Paleoceanography 11 (1996) 467–480.

[15] S. Al-Rousan, S. Al-Moghrabi, J. Pätzold, G. Wefer, Stable oxygen isotopes in *Porites* corals monitor weekly temperature variations in the northern Gulf of Aqaba, Red Sea, Coral Reefs 22 (2003) 346–356.

[16] B.K. Linsley, R.B. Dunbar, G.M. Wellington, D.A. Mucciarone, A coral based reconstruction of Intertropical Convergence Zone variability over Central-America since 1707, J. Geophys. Res. 99 (1994) 9977–9994.
[17] A.W. Tudhope, G.B. Shimmield, C.P. Chilcott, M. Jebb, A.E. Fallick, A.N. Dalgleish, Recent changes in climate in the far western equatorial Pacific and their relationship to the Southern Oscillation; Oxygen isotope records from massive corals, Papua New Guinea, Earth Planet. Sci. Lett. 136 (1995) 575–590.
[18] N. Le Bec, A. Juillet-Leclerc, T. Corrège, D. Blamart, T. Delcroix, A coral $\delta^{18}O$ record of ENSO driven sea surface salinity variability in Fiji (south-western tropical Pacific), Geophys. Res. Lett. 27 (2000) 3897–3900.
[19] J.D. Carriquiry, M.J. Risk, H.P. Schwarcz, Stable-isotope geochemistry of corals from Costa-Rica as proxy indicator of the El-Niño Southern Oscillation (ENSO), Geochim. Cosmochim. Acta 58 (1994) 335–351.
[20] M.K. Gagan, L.K. Ayliffe, D. Hopley, J.A. Cali, G.E. Mortimer, J. Chappell, M.T. McCulloch, M.J. Head, Temperature and surface-ocean water balance of the mid-Holocene tropical Western Pacific, Science 279 (1998) 1014–1018.
[21] J.W. Beck, R.L. Edwards, E. Ito, F.W. Taylor, J. Recy, F. Rougerie, P. Joannot, C. Henin, Sea-surface temperature from coral skeletal strontium calcium ratios, Science 257 (1992) 644–647.
[22] C. Alibert, M.T. McCulloch, Strontium/calcium ratios in modern *Porites* corals from the Great Barrier Reef as a proxy for sea surface temperature: calibration of the thermometer and monitoring of ENSO, Paleoceanography 12 (1997) 345–363.
[23] J.F. Marshall, M.T. McCulloch, An assessment of the Sr/Ca ratio in shallow water hermatypic corals as a proxy for sea surface temperature, Geochim. Cosmochim. Acta 66 (2002) 3263–3280.
[24] H.M. Stoll, D.P. Schrag, Effects of Quaternary sea level cycles on strontium in seawater, Geochim. Cosmochim. Acta 62 (1998) 1107–1118.
[25] H.M. Stoll, D.P. Schrag, S.C. Clemens, Are seawater Sr/Ca variations preserved in Quaternary foraminifera? Geochim. Cosmochim. Acta 63 (1999) 3535–3547.
[26] K.A. Hughen, D.P. Schrag, S.B. Jacobsen, W. Hantoro, El Niño during the last interglacial period recorded by a fossil coral from Indonesia, Geophys. Res. Lett. 26 (1999) 3129–3132.
[27] M.T. McCulloch, A.W. Tudhope, T.M. Esat, G.E. Mortimer, J. Chappell, B. Pillans, A.R. Chivas, A. Omura, Coral record of equatorial sea-surface temperatures during the penultimate deglaciation at Huon Peninsula, Science 283 (1999) 202–204.
[28] A.W. Tudhope, C.P. Chilcott, M.T. McCulloch, E.R. Cook, J. Chappell, R.M. Ellam, D.W. Lea, J.M. Lough, G.B. Shimmield, Variability in the El Niño-Southern Oscillation through a glacial–interglacial cycle, Science 291 (2001) 1511–1517.
[29] T. Felis, G. Lohmann, H. Kuhnert, S.J. Lorenz, D. Scholz, J. Pätzold, S.A. Al-Rousan, S.M. Al-Moghrabi, Increased seasonality in Middle East temperatures during the last interglacial period, Nature 429 (2004) 164–168.
[30] Y.A. Moustafa, J. Pätzold, Y. Loya, G. Wefer, Mid-Holocene stable isotope record of corals from the northern Red Sea, Int. J. Earth Sci. 88 (2000) 742–751.
[31] A. Suzuki, M.K. Gagan, P. De Deckker, A. Omura, I. Yukino, H. Kawahata, Last Interglacial coral record of enhanced insolation seasonality and seawater ^{18}O enrichment in the Ryukyu Islands, northwest Pacific, Geophys. Res. Lett. 28 (2001) 3685–3688.
[32] K.H. Kilbourne, T.M. Quinn, F.W. Taylor, A fossil coral perspective on western tropical Pacific climate ~ 350 ka, Paleoceanography 19 (2004), doi: 10.1029/2003PA000944.
[33] T.C. Brachert, M. Reuter, T. Felis, K.F. Kroeger, G. Lohmann, A. Micheels, C. Fassoulas, *Porites* corals from Crete (Greece) open a window into Late Miocene (10 Ma) seasonal and interannual climate variability, Earth Planet. Sci. Lett. 245 (2006) 81–94.
[34] A. Winter, A. Paul, J. Nyberg, T. Oba, J. Lundberg, D. Schrag, B. Taggart, Orbital control of low-latitude seasonality during the Eemian, Geophys. Res. Lett. 30 (2003), doi: 10.1029/2002GL016275.
[35] D. Sun, M.K. Gagan, H. Cheng, H. Scott-Gagan, C.A. Dykoski, R.L. Edwards, R. Su, Seasonal and interannual variability of the mid-Holocene East Asian monsoon in coral $\delta^{18}O$ records from the South China Sea, Earth Planet. Sci. Lett. 237 (2005) 69–84.
[36] J.R. Petit, J. Jouzel, D. Raynaud, N.I. Barkov, J.M. Barnola, I. Basile, M. Bender, J. Chappellaz, M. Davis, G. Delaygue, M. Delmotte, V.M. Kotlyakov, M. Legrand, V.Y. Lipenkov, C. Lorius, L. Pepin, C. Ritz, E. Saltzman, M. Stievenard, Climate and atmospheric history of the past 420,000 years from the Vostok ice core, Antarctica, Nature 399 (1999) 429–436.
[37] R.M. Carter, P. Gammon, New Zealand maritime glaciation: Millennial-scale southern climate change since 3.9 Ma, Science 304 (2004) 1659–1662.
[38] C.H. Stirling, T.M. Esat, K. Lambeck, M.T. McCulloch, S.G. Blake, D.C. Lee, A.N. Halliday, Orbital forcing of the marine isotope stage 9 interglacial, Science 291 (2001) 290–293.
[39] T.G. Benton, T. Spencer, Biogeographic processes at the limits of the Indo-West Pacific Province, Biol. J. Linn. Soc. 56 (1995) 243–244.
[40] R.A. Irving, Near-shore bathymetry and reef biotopes of Henderson Island, Pitcairn Group, Biol. J. Linn. Soc. 56 (1995) 309–324.
[41] J.M. Pandolfi, Geomorphology of the uplifted Pleistocene atoll at Henderson Island, Pitcairn Group, Biol. J. Linn. Soc. 56 (1995) 63–77.
[42] S.G. Blake, Late Quaternary history of Henderson Island, Pitcairn Group, Biol. J. Linn. Soc. 56 (1995) 43–62.
[43] W.G. Thompson, M.W. Spiegelman, S.L. Goldstein, R.C. Speed, An open-system model for U-series age determinations of fossil corals, Earth Planet. Sci. Lett. 210 (2003) 365–381.
[44] M.B. Andersen, C.H. Stirling, E.-K. Potter, A.N. Halliday, S. Blake, M. McCulloch, B. Ayling, M. O'Leary, A record of multiple sea-level high-stands for the last 650 ka preserved at Henderson Island, a coral atoll in the South Pacific, EOS Transactions, AGU Fall Meet. Suppl. 85 (2004) (Abstract U31A 0010).
[45] M.B. Andersen, C.H. Stirling, E.-K. Potter, A.N. Halliday, Toward epsilon levels of measurement precision on $^{234}U/^{238}U$ by using MC-ICPMS, Int. J. Mass Spectrom. 237 (2004) 107–118.
[46] E.-K. Potter, C.H. Stirling, M.B. Andersen, A.N. Halliday, High precision Faraday collector MC-ICPMS thorium isotope ratio determination, Int. J. Mass Spectrom. 247 (2005) 10–17.
[47] H. Cheng, R.L. Edwards, J. Hoff, C.D. Gallup, D.A. Richards, Y. Asmerom, The half-lives of uranium-234 and thorium-230, Chem. Geol. 169 (2000) 17–33.
[48] S. Levitus, R. Burgett, T.P. Boyer, World Ocean Atlas, Salinity, NOAA Atlas, National Environmental Satellite Data Information Service 3, vol. 3, U.S. Department of Commerce, Washington, D.C., 1994, p. 99.
[49] M.K. Gagan, A.R. Chivas, P.J. Isdale, High-resolution isotopic records from corals using ocean temperature and mass spawning chronometers, Earth Planet. Sci. Lett. 121 (1994) 549–558.
[50] D.J. Sinclair, High spatial-resolution analysis of trace elements in corals using laser ablation ICP-MS, PhD, Australian National University, 1998.
[51] S.J. Fallon, M.T. McCulloch, R. van Woesik, D.J. Sinclair, Corals at their latitudinal limits: laser ablation trace element

systematics in *Porites* from Shirigai Bay, Japan, Earth Planet. Sci. Lett. 172 (1999) 221–238.
[52] T. Mitsuguchi, E. Matsumoto, O. Abe, T. Uchida, P.J. Isdale, Mg/Ca thermometry in coral-skeletons, Science 274 (1996) 961–963.
[53] A. Suzuki, I. Yukino, H. Kawahata, Temperature–skeletal $\delta^{18}O$ relationship of *Porites australiensis* from Ishigaki Island, the Ryukyus, Japan, Geochem. J. 33 (1999) 419–428.
[54] R. Asami, T. Yamada, Y. Iryu, C.P. Meyer, T.M. Quinn, G. Paulay, Carbon and oxygen isotopic composition of a Guam coral and their relationships to environmental variables in the western Pacific, Palaeogeogr. Palaeoclimatol. Palaeoecol. 212 (2004) 1–22.
[55] G.M. Wellington, R.B. Dunbar, Stable isotopic signature of El-Niño Southern Oscillation events in eastern tropical Pacific reef corals, Coral Reefs 14 (1995) 5–25.
[56] K.F. Yu, J.X. Zhao, G.J. Wei, X.R. Cheng, T.G. Chen, T. Felis, P.X. Wang, T.S. Liu, $\delta^{18}O$, Sr/Ca and Mg/Ca records of *Porites lutea* corals from Leizhou Peninsula, northern South China Sea, and their applicability as paleoclimatic indicators, Palaeogeogr. Palaeoclimatol. Palaeoecol. 218 (2005) 57–73.
[57] M.K. Gagan, A.R. Chivas, Oxygen isotopes in western Australian coral reveal Pinatubo aerosol-induced cooling in the Western Pacific Warm Pool, Geophys. Res. Lett. 22 (1995) 1069–1072.
[58] C.L. Stephans, T.M. Quinn, F.W. Taylor, T. Corrège, Assessing the reproducibility of coral-based climate records, Geophys. Res. Lett. 31 (2004), doi: 10.1029/2004GL020343.
[59] T.M. Quinn, T.J. Crowley, F.W. Taylor, C. Henin, P. Joannot, Y. Join, A multicentury stable isotope record from a New Caledonia coral: Interannual and decadal sea surface temperature variability in the southwest Pacific since 1657 AD, Paleoceanography 13 (1998) 412–426.
[60] T.M. Quinn, F.W. Taylor, T.J. Crowley, S.M. Link, Evaluation of sampling resolution in coral stable isotope records: A case study using records from New Caledonia and Tarawa, Paleoceanography 11 (1996) 529–542.
[61] S. de Villiers, G.T. Shen, B.K. Nelson, The Sr/Ca-temperature relationship in coralline aragonite: Influence of variability in $(Sr/Ca)_{seawater}$ and skeletal growth parameters, Geochim. Cosmochim. Acta 58 (1994) 197–208.
[62] C.-C. Shen, T. Lee, C.-Y. Chen, C.-H. Wang, C.-F. Dai, L.-A. Li, The calibration of $D_{(Sr/Ca)}$ versus sea surface temperature relationship for *Porites* corals, Geochim. Cosmochim. Acta 60 (1996) 3849–3858.
[63] B.K. Linsley, G.M. Wellington, D.P. Schrag, Decadal sea surface temperature variability in the subtropical South Pacific from 1726 to 1997 AD, Science 290 (2000) 1145–1148.
[64] T. Corrège, M.K. Gagan, W.J. Beck, G.S. Burr, G. Cabioch, F. Le Cornec, Interdecadal variation in the extent of South Pacific tropical waters during the Younger Dryas event, Nature 428 (2004) 927–929.
[65] J.F. Marshall, M.T. McCulloch, Evidence of El Niño and the Indian Ocean Dipole from Sr/Ca derived SSTs for modern corals at Christmas Island, Eastern Indian Ocean, Geophys. Res. Lett. 28 (2001) 3453–3456.
[66] W.J. Beck, J. Recy, F. Taylor, R.L. Edwards, G. Cabioch, Abrupt changes in early Holocene tropical sea surface temperatures derived from coral records, Nature 385 (1997) 705–707.
[67] T.M. Quinn, D.E. Sampson, A multiproxy approach to reconstructing sea surface conditions using coral skeleton geochemistry, Paleoceanography 17 (2002), doi: 10.1029/2000PA000528.
[68] T. Corrège, T. Delcroix, J. Recy, W. Beck, G. Cabioch, F. Le Cornec, Evidence for stronger El Niño-Southern Oscillation (ENSO) events in a mid-Holocene massive coral, Paleoceanography 15 (2000) 465–470.
[69] C. Perrin, Compositional heterogeneity and microstructural diversity of coral skeletons: implications for taxonomy and control on early diagenesis, Coral Reefs 22 (2003) 109–120.
[70] C. Perrin, J.-P. Cuif, Ultrastructural controls on diagenetic patterns on scleractinian skeletons: evidence at the scale of a colony lifetime, Bull. Tohoku Univ. Mus. 1 (2001) 210–218.
[71] J.-P. Cuif, Y. Dauphin, The two-step mode of growth in the scleractinian coral skeletons from the micrometre to the overall scale, J. Struct. Biol. 150 (2005) 319–331.
[72] G.T. Shen, R.B. Dunbar, Environmental controls on uranium in reef corals, Geochim. Cosmochim. Acta 59 (1995) 2009–2024.
[73] G.R. Min, R.L. Edwards, F. Taylor, J. Recy, C.D. Gallup, W.J. Beck, Annual cycles of U/Ca in coral skeletons and U/Ca thermometry, Geochim. Cosmochim. Acta 59 (1995) 2025–2042.
[74] A.L. Cohen, R.A. Sohn, Tidal modulation of Sr/Ca ratios in a Pacific reef coral, Geophys. Res. Lett. 31 (2004), doi: 10.1029/2004GL020600.
[75] A.L. Cohen, K.E. Owens, G.D. Layne, N. Shimizu, The effect of algal symbionts on the accuracy of Sr/Ca paleotemperatures from coral, Science 296 (2002) 331–333.
[76] A.L. Cohen, G.D. Layne, S.R. Hart, P.S. Lobel, Kinetic control of skeletal Sr/Ca in a symbiotic coral: Implications for the paleotemperature proxy, Paleoceanography 16 (2001) 20–26.
[77] S.V. Smith, R.W. Buddemeier, R.C. Redalje, J.E. Houck, Strontium–calcium thermometry in coral skeletons, Science 204 (1979) 404–407.
[78] D. Paillard, L. Labeyrie, P. Yiou, Analyseries 1.0: A Macintosh software for the analysis of geographical time series, EOS Trans. 7 (1996) 379.
[79] S. Levitus, A comparison of the annual cycle of two sea surface temperature climatologies of the world ocean, J. Phys. Oceanogr. 17 (1987) 197–214.
[80] I.M. Yashayaev, I.I. Zveryaev, Climate of the seasonal cycle in the north Pacific and the north Atlantic oceans, Int. J. Climatol. 21 (2001) 401–417, doi: 10.1002/joc.585.